

Casimir nanoparticle levitation in vacuum with broadband perfect magnetic conductor metamaterials

Adrián E. Rubio López^{1,*} and Vincenzo Giannini^{2,3,4}

¹*Birck Nanotechnology Center, School of Electrical and Computer Engineering,
Purdue University, West Lafayette, IN 47907, USA*

²*Technology Innovation Institute, P.O. Box 9639,
Building B04C, Masdar City, Abu Dhabi, United Arab Emirates*

³*Instituto de Estructura de la Materia (IEM-CSIC),
Consejo Superior de Investigaciones Científicas, Serrano 121, 28006 Madrid, Spain*

⁴*Centre of Excellence ENSEMBLE3 Sp. z o. o.,
Wolczynska Str. 133, 01-919, Warsaw, Poland[†]*

(Dated: October 24, 2022)

The levitation of nanoparticles is essential in various branches of research. Casimir forces are natural candidates to tackle it but the lack of broadband metamaterials precluded repulsive forces in vacuum. We show sub-micron nanoparticle levitation in vacuum only based on the design of a broadband metamaterial perfect magnetic conductor surface, where the force is mostly given by the (quantum) zero-point contribution. In the harmonic regime of the center of mass dynamics, the characteristic frequency depends linearly on Planck's constant \hbar while independent of the nanoparticle's volume.

Levitation is an intriguing physical phenomenon that could majorly impact our daily life; a typical example is magnetically levitated trains. Currently, different approaches for levitating objects of different shapes, sizes and materials, and also under a broad variety of scenarios were investigated [1–8]. Some approaches exploit the repulsive electric forces perceived by charges of the same sign, while others are based on employing optical potentials or tweezers. Because of its high controllability and hybrid properties, levitated nanoparticles in highly isolated scenarios are objects of high interest since its impact in both technological applications and fundamental science. Given their rich phenomenology, nanoparticles are sensitive to fluctuation phenomena, such as Casimir-Polder forces. The latter were broadly studied as a possible advantageous levitation mechanism [9–16], but strong limitations were found on narrow bandwidths of the materials involved (either for ordinary materials or metamaterials) [17–21], or the necessity of liquid immersion of the interacting bodies [22–24]. Nevertheless, a successful realization in vacuum may lead to a new generation of experiments and applications characterized by minimalistic setups and extreme nanoparticle's isolation.

In this Letter we demonstrate the levitation of nanoparticles in vacuum at arbitrary temperature on a sub-micron distance by simply exploiting Casimir interactions with a broadband perfect magnetic conductor (PMC) metamaterial plane surface. We also suggest a possible way to realize such metamaterial.

Taking advantage from the natural repulsive interaction between point objects, such as charges and dipoles, with a PMC surface, we show that even when the PMC property is restricted to a finite bandwidth, but enough broad, excluding high and low frequencies, the repulsive condition of the force is preserved while its magnitude

presents modest variations with respect to the full-band or perfect PMC surface. By opposing this force to the nanoparticle's weight, we show stable levitation for different nanoparticle's materials. For small nanoparticles, we show that the levitation dynamics is independent of its volume. Since the stable point takes place at the sub-micron scale, the Casimir-Polder force is mostly given by the quantum fluctuation or zero temperature contribution. Thus, the levitation mechanism results robust to thermal effects. Given the asymmetry on the total potential, anharmonic periodic motion is obtained for nanoparticle's energies well above the potential's minima. For energies close to the minima, the dynamics is effectively harmonic, and characterized by a frequency linearly dependent on Planck's constant \hbar and independent of the nanoparticle's volume. The quantum nature of this phenomenon can be recognized by the oscillation frequency dependence on \hbar .

Specifically, we consider a spherical nanoparticle of mass density ρ and radius $R = 50$ nm, such that its mass $m = \rho V$ (being $V = 4\pi R^3/3$ its volume). Nanoparticles of this radius are well described as electric point-dipoles. Their polarizability is given by Clausius-Mossotti formula $\alpha(\omega) = V\xi(\omega)$, with $\xi(\omega) = 3[\varepsilon(\omega) - 1]/[\varepsilon(\omega) + 2]$ the polarizability per unit volume, being $\varepsilon(\omega)$ the nanoparticle's material permittivity. The nanoparticle is placed at a distance z from a plane surface. The surface is assumed made of a metamaterial with PMC properties over some finite range of frequencies; we suggest how to build such a metamaterial, ultimately characterized by its reflection and transmission coefficients for the transverse-electric and -magnetic (TE and TM, $\{r_{s,p}, t_{s,p}\}$) modes, respectively. A scheme is presented on Fig.1a. The physical intuition about a nanoparticle interacting with a PMC plane is obtained considering basic objects as charges

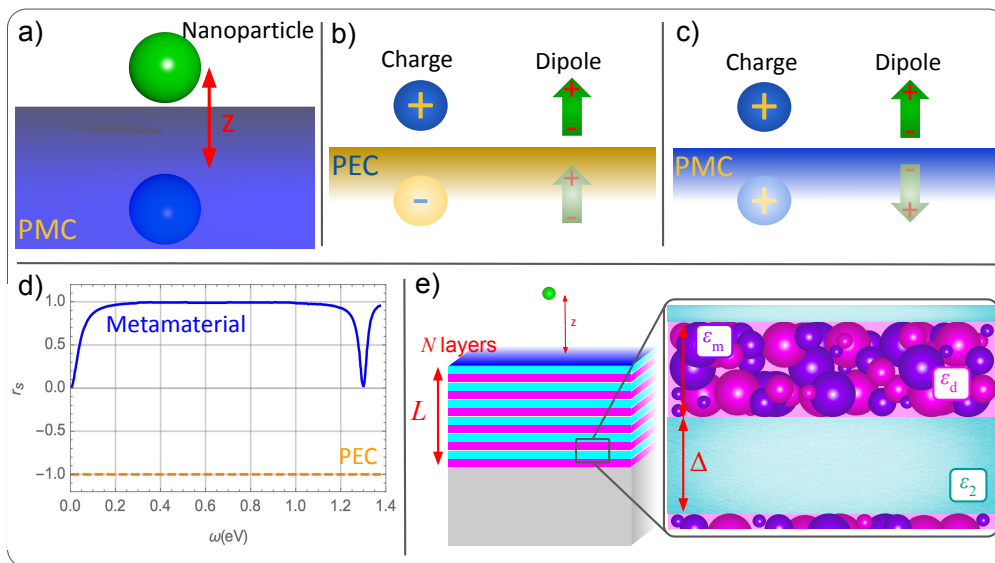


FIG. 1. a) Scheme of the scenario. As the nanoparticle is effectively considered a point-dipole, the configuration stands for a Casimir-Polder scenario. b,c) Scheme of the physical intuition of the differences between the interaction of basic objects (charges and dipoles) with a perfect conductor surface. For the PEC case, the charge has an image-charge with the opposite sign. For the PMC case, the charge has an image-charge preserves the sign of the original, the dipole results in a mirror image. While the force is attractive for the PEC case, for the PMC is repulsive. d) Comparison between the reflection coefficients of a PEC plane and the quasi PMC plane presented in this work. The PEC presents an ideal reflection coefficient $r_s = -1$ at every frequency of the spectrum. On the other hand, the metamaterial behaves as a PMC within an extended bandwidth, where $r_s \simeq 1$. e) Scheme of the quasi PMC made with 1000 pairs of layers with thicknesses $\Delta_1 = \Delta_2 \equiv \Delta = 5$ nm and permittivities $\epsilon_1 = -5$ and $\epsilon_2 = +5$. The negative constant permittivity is the effective ϵ of a composite made of metal (ϵ_m) and insulator (ϵ_d) nanoparticles. Reflection coefficients obtained with a transfer matrix approach.

and dipoles in the static case. The method of images gives a clear insight for the basic scenarios, shown in the lower panels of Fig.1. In analogy to a PEC, where the boundary conditions are $\hat{n} \times \mathbf{E} = 0$ (with \hat{n} the normal direction to the boundary and \mathbf{E} the electric field), for the PMC we have $\hat{n} \times \mathbf{B} = 0$. These boundary conditions imply (for any incident angle and frequency) that for a PEC we have $r_s = -r_p = -1$ while for a PMC $r_s = -r_p = +1$. A striking consequence of this is that while a positive charge interacts with a PEC surface with a negative mirror-charge, for the PMC the mirror-charge is positive. This implies that the force between the PEC and a charge is attractive, while for the PMC results repulsive. The same intuition is extended to the case of electric dipoles, which gives an insight of what is expected for nanoparticles, although the latter are fluctuating objects. For nanoparticle levitation the spectral broadness of the PMC property is the key-point. Previous works, in fact, have questioned the possibility of including magnetic resonant metamaterials in Casimir physics [17, 19, 20]. The conclusion was that the magnetic properties of resonant metamaterials do not have enough spectral broadness, precluding a concrete realization. Metamaterials were taking their properties from their component's resonant nature, which implies that the magnetic behavior was limited to a narrow frequency

region but was not enough to obtain levitation or repulsive effects. Another important limiting factor they found is the presence of losses in the metamaterial [19].

Here we take another approach. We design a long wavelength metamaterial, i.e., a material that have the desired properties when the photon wavelength λ is much larger than the characteristic spatial scales of the metamaterials (for example, the unit cell in a periodic system). In this way, we avoid having a functional material working only on a narrow frequency band, as in resonant metamaterials. These kind of ideas have been recently applied in order to obtain metallic transparent metamaterials [25, 26]. In this way, we can obtain a quasi-PMC, i.e., a metamaterial behaving as a PMC in a broad range of frequencies. For this, first, we elucidate what should be the properties of a planar multi-layer array that behaves as a PCM, and secondly, we suggest a possible way to fabricate such a system. We also would like to point out that our main aim is to show that there is no fundamental restriction against a broadband PMC.

It is possible to show (see Sect.I of the Suppl.Mat. and section 1.6.2 from [27]) that the normal incidence reflection coefficient, r_s , of a stratified medium of N thin films with thickness Δ_n ($\Delta_n \ll \lambda$) in air, is given by:

$$r_s = \frac{ik(A - B)}{2 - ik(A + B)}, \quad (1)$$

where $k = 2\pi/\lambda = \omega/c$, $A = \sum_n^N \varepsilon_n \Delta_n$ and $B = \sum_n^N \mu_n \Delta_n$, being ε_n and μ_n the relative permittivity and permeability of the n -th layer. If our layers are not magnetic ($\mu_n = 1$), then $B = L$, being L the total multi-layer thickness. We can also choose materials and thicknesses such that $A \sim 0$, obtaining for $kL \gg 1$:

$$r_s = \frac{-ikL}{2 - ikL} \approx +1. \quad (2)$$

In other words, the requirements for a stratified medium of thin films to behave effectively as a PMC are $A \sim 0$ and $kL \gg 1$.

In order to verify our hypothesis, we consider here a representative example. We calculated the exact reflection coefficient of 1000 pairs of films ($N = 2000$) with thicknesses $\Delta_1 = \Delta_2 \equiv \Delta = 5\text{nm}$ (see Fig.1e) and permittivities $\varepsilon_1 = -5$ and $\varepsilon_2 = +5$ obtaining $A = (\Delta_1 \varepsilon_1 + \Delta_2 \varepsilon_2)N/2 = 0$. Using a transfer matrix method, we show the result in Fig.1d together with the reflection coefficient for a PEC. We can appreciate that $r_s \approx +1$ in a broad range of frequencies confirming our prediction. The multi-layer deviates from a PMC at low energies when $\lambda \sim L$ and at high energy when the wavelength inside the medium is comparable with the thicknesses Δ_n . The lower frequency limit can be improved just having metamaterials with much larger L , while the high energy limit can be improved having thinner films.

Until now, we analyzed the behavior of the multi-layer at normal incidence. Nevertheless, the reflectivity at any frequency and parallel wave-vector k_{\parallel} is required. A simple way to obtain it is recurring to the effective properties of a multi-layer system [28, 29]. The effective dielectric constant along the z axis perpendicular to the planes reads:

$$\varepsilon_z = \frac{\Delta_1 + \Delta_2}{\Delta_1/\varepsilon_1 + \Delta_2/\varepsilon_2}, \quad (3)$$

while the in-plane dielectric constants reads:

$$\varepsilon_x = \varepsilon_y = \frac{\varepsilon_1 \Delta_1 + \varepsilon_2 \Delta_2}{\Delta_1 + \Delta_2}. \quad (4)$$

Assuming same thickness and opposite dielectric constants, we obtain $\varepsilon_z \approx \pm\infty$ and $\varepsilon_x = \varepsilon_y \approx 0$. With these values and the reflection coefficients of an anisotropic plane [30]

$$r_s = \frac{\sqrt{\omega/c - k_{\parallel}^2} - \sqrt{\varepsilon_x \omega/c - k_{\parallel}^2}}{\sqrt{\omega/c - k_{\parallel}^2} + \sqrt{\varepsilon_x \omega/c - k_{\parallel}^2}}, \quad (5)$$

and

$$r_p = \frac{\varepsilon_x \sqrt{\omega/c - k_{\parallel}^2} - \sqrt{\varepsilon_x \omega/c - \varepsilon_x k_{\parallel}^2 / \varepsilon_z}}{\varepsilon_x \sqrt{\omega/c - k_{\parallel}^2} + \sqrt{\varepsilon_x \omega/c - \varepsilon_x k_{\parallel}^2 / \varepsilon_z}}, \quad (6)$$

we obtain $r_p \approx -1$ and $r_s \approx 1 - \chi$ where the correction χ to 1 for r_s is given by

$$\chi = 2i \sqrt{\frac{k_{\parallel}^2}{k^2} \left(1 - \frac{k_{\parallel}^2}{k^2}\right) + 2 \frac{k_{\parallel}^2}{k^2}}, \quad (7)$$

we can appreciate that at a normal incidence we have $r_s \approx +1$ and for big values of k_{\parallel} we have $r_s \approx 0$. These reflection coefficients will be used later to calculate the Casimir force acting on a nanoparticle above the metamaterial.

At this point, we comment on how materials with ε constant and negative in a broad range of frequencies are obtained. Materials with positive constant ε in a wide range of frequencies are easily found in nature (insulators). However, we cannot directly find materials with constant negative permittivity. For instance, metals do not have constant values of ε with the frequency. A possible solution is to consider the composite of metal and insulators and the fascinating physics of percolating systems [31]. The permittivity of aggregates made of small spherical inclusions of two phases (see Fig.1e), conductive (ε_m) and insulator (ε_d), can be described in good approximation by the Bruggeman and Landauer self-consistent (SC) approximation when both phases can be treated symmetrically [31], i.e. when they are invariant to simultaneous interchange of the phase conductivities and volume fractions. In particular, if one of the two phases is a good metal, we have that $|\varepsilon_m| \gg \varepsilon_d$ in a broad range of wavelengths starting from the visible zone. This leads to find a simple expression for the effective permittivity [32]:

$$\varepsilon_{\text{eff}} = \frac{\varepsilon_d}{1 - 3\phi_m}, \quad (8)$$

where ϕ_m is the metallic volume fraction [31]. As pointed out by Landauer, for values of ϕ_m above the percolation threshold, $\phi_c = 1/3$, we obtain a metallic behavior. A composite with two phases of large permittivity contrast and where the above expression works accurately, have usually a fractal structure [33, 34], while in general some deviation is found [31]. In particular, an approach relevant to our goals has been shown by M. Hövel *et al.* studying the insulator-to-metal transition in thin metallic films [35]. They observed that the thickness of the film could be used to "tweak" such transition and measured constant dielectric negative permittivities for frequencies starting in the visible/near-infrared up to zero frequency. In addition, the constant behavior of the permittivity implies negligible absorption (imaginary part of $\varepsilon_{\text{eff}} \approx 0$), because the Kramers-Kronig relations connect real and imaginary parts. Such results are extremely relevant to our proposal.

All in all, for wavelengths of hundred of nanometers (much larger than the unit cell), the metamaterial made with thin films shows effective reflective properties as

shown in Fig.1d. In contrast to a PEC plane, the metamaterial shows an effective PMC reflection $r_s \simeq 1$ for a broad region. This has a crucial impact on the Casimir-Polder force acting on a nanoparticle.

The force on a nanoparticle arises from the interaction between the surrounding EM field, the plane surface and the nanoparticle considered as a point dipole. A detailed derivation is shown in Sect.II of the Suppl. Mat. By following Refs.[36, 37], the force over the dipole reads to the lowest order in perturbation theory reads:

$$\mathbf{F}(\mathbf{r}) \approx \left\langle \hat{d}_i^{(\text{ind})}(t) \nabla \hat{E}_i^{(\text{fl})}(\mathbf{r}, t) \right\rangle + \left\langle \hat{d}_i^{(\text{fl})}(t) \nabla \hat{E}_i^{(\text{ind})}(\mathbf{r}, t) \right\rangle, \quad (9)$$

where \mathbf{r} stands for the nanoparticle's position and summation over latin subscripts is implicit. The first term describes the fluctuations of the field that correlate with the corresponding induced dipole, while the second involves dipole fluctuations and the field they induce. In principle, each entity is assumed to have its own temperature, $\{T_{\text{EM}}, T_{\text{S}}, T_{\text{NP}}\}$. The force acting on the nanoparticle at a distance z from the surface for a general nonequilibrium scenario can be splitted according to the surface reflection and transmission properties:

$$F_z(z) = F_0(z) + F_{\text{R}}(z, T_{\text{EM}}, T_{\text{NP}}) + F_{\text{T}}(z, T_{\text{EM}}, T_{\text{S}}), \quad (10)$$

where F_0 stands for the contribution of the zero-point fluctuations, which depends on the surface's reflection coefficients $\{r_{s,p}\}$; F_{R} stands for the contribution associated to the surrounding EM field and the nanoparticle radiation and it also depends on the reflection coefficients, while F_{T} relates to the radiation of the surface and depends exclusively on the surface's transmission coefficients $\{t_{s,p}\}$. A metamaterial surface described by Eqs.(5)-(7) may present frequency cutoffs. We refer as 'full-bandwidth' cases as the ones where reflection and transmission properties do not present any frequency cutoffs. For a perfect conductor, there are two possibilities: PEC and PMC. For the full-bandwidth PEC (PMC) surface that $r_s \rightarrow \mp 1$, $r_p \rightarrow \pm 1$, while $t_{s,p} \rightarrow 0$ for every $\{\omega, k_{\parallel}\}$. The latter implies that $F_{\text{T}} \rightarrow 0$ regardless on the temperatures. In agreement to the intuitive picture of Fig. 1, in Sect.III of the Suppl. Mat. we show the striking feature $F_z^{(\text{PMC})} = -F_z^{(\text{PEC})}$. In principle, this theoretically guarantees the levitation of a nanoparticle at a certain distance provided the full-bandwidth PMC property is effective. However, our proposed metamaterial presents PMC properties on finite bandwidth according to Fig. 1e and Eqs.(5)-(7).

For a nanoparticle of 50nm radius, the weight is in the orders of $mg \sim 10^{-17}\text{N}$ for common materials such as SiC, Au and Si. Levitation is possible at distances where the Casimir-Polder force compensates the weight. As we show below, this occurs for $z < 1\mu\text{m}$. In the short-distance regime, for which $k_{\text{B}}T_{\text{Min}}z/[hc] \ll 1$ (with $T_{\text{Min}} = \min[T_{\text{Env}}, T_{\text{NP}}]$), the Casimir-Polder force is given

by the zero-temperature (fully quantum) contribution [see Eqs.(S.53-S.55) of the Suppl. Mat. for the full expression]:

$$F_z(z) \approx F_0(z). \quad (11)$$

This implies that the conclusions obtained from now are robust to thermal (and nonequilibrium) effects and relies on the (quantum) zero-point fluctuations (see Sect.IVA of the Suppl. Mat.). For the full-bandwidth PMC, the zero-temperature contribution to the force reads:

$$F_0(z) \rightarrow F_0^{(\text{PMC})}(z) = 3\hbar V I_0(z)/(8\pi z^4), \quad (12)$$

which is independent of V , having $I_0(z) \equiv \int_0^{+\infty} \frac{d\omega}{2\pi} \xi(i\omega) A(i\omega, z) e^{-2\frac{\omega}{c}z}$, with $A(i\omega, z) = \sum_{n=0}^3 \frac{1}{n!} (2\frac{\omega}{c}z)^n$. In Fig. 2 we show the Casimir-Polder force acting on a SiC nanoparticle of 50 nm radius for different upper and lower frequency cutoffs combinations. For SiC we employed a permittivity model $\varepsilon_{\text{SiC}}(\omega) = \varepsilon_{\infty}(\omega_{\text{L}}^2 - \omega^2 - i\gamma\omega)/(\omega_{\text{T}}^2 - \omega^2 - i\gamma\omega)$, where $\omega_{\text{L}} = 18.253 \cdot 10^{13}\text{s}^{-1}$, $\omega_{\text{T}} = 14.937 \cdot 10^{13}\text{s}^{-1}$, $\gamma = 8.966 \cdot 10^{11}\text{s}^{-1}$ and $\varepsilon_{\infty} = 6.7$. The nanoparticle is positioned on the multi-layer system as shown in Fig. 1e. According to the basic physical intuition described for a PMC in Fig. 1, a repulsive force should act on the nanoparticle if we have a broadband PMC. A broader interval in frequencies increases the repulsion at every distance from the surface. The maximum repulsion should be achieved for the full-bandwidth PCM (ideal case). This is confirmed in Fig. 2 (blue solid curve),

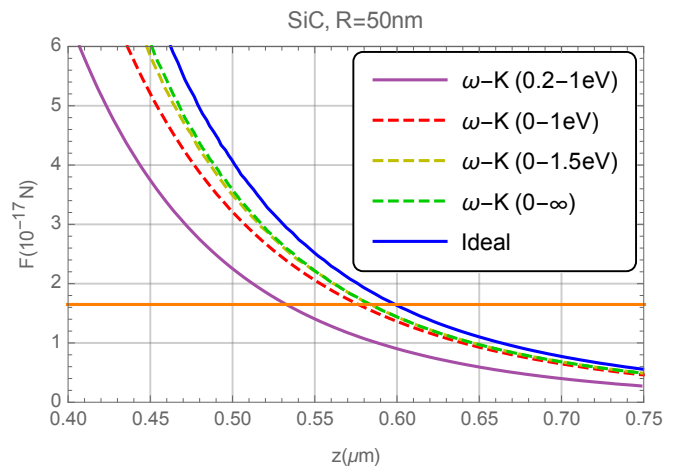


FIG. 2. Casimir-Polder for acting on a SiC nanoparticle with $R = 50$ nm radius for different upper and lower cutoffs. The force is given by Eq.(11) in combination with the reflection coefficients on Eqs. (5) and (6) for the system shown in Fig. 1e. The orange solid horizontal line corresponds to the nanoparticle's weight mg . The intersections between the weight and the different curves give the levitation position for each case, where the Casimir-Polder repulsion is compensated by the weight (with opposite sign).

while a small reduction is observed if we use the reflection coefficients given by Eqs. (5) and (6) without cutoffs (green dashed curve). In Sect.III of Suppl. Mat., it is shown that for a SiC nanoparticle we have that $I_0(z) \approx 3c(\varepsilon_\infty - 1)/[\pi z(\varepsilon_\infty + 2)]$ for $z \approx z_0$ with a difference of 3% with respect to the actual value. Then, we also show that for a SiC nanoparticle the force by a full-bandwidth PMC surface $F_0^{(\text{PMC})}$ (blue solid curve) or by a full-bandwidth metamaterial surface $F_0^{(\text{FM})}$ (green dashed curve) can be approximated respectively by:

$$F_0^{(\text{PMC})}(z) \approx \frac{9\hbar cV}{8\pi^2 z^5} \frac{(\varepsilon_\infty - 1)}{(\varepsilon_\infty + 2)}, \quad (13)$$

$$F_0^{(\text{FM})}(z) \approx \left(\frac{5}{3} - \frac{\pi}{4}\right) F_0^{(\text{PMC})}(z), \quad (14)$$

giving a difference close to 11% between the full-bandwidth cases, as it is shown numerically in Fig.2. Furthermore, we also show that when cutoffs are considered a repulsion reduction is observed, as expected. The differences with respect to the full-bandwidth case are not critical. We also checked that in the worst scenario (i.e., for which the metamaterial is assumed to behave as a PEC outside the cutoffs) the total force is still repulsive, with a small deviation from Fig. 2. This allow us to take the full-bandwidth PMC case as representative for our analysis. In other words, the presented metamaterial with a realistic bandwidth is mostly approximated by the scenario of a full-bandwidth PMC. From now on, we focus on the latter for continuing the analysis, while considering that a finite bandwidth effectively decreases the force at each position in a moderate magnitude. A striking feature is that in all the cases the nanoparticle's weight (orange solid line, taking $\rho = 3210\text{Kg/m}^3$) is compensated by the Casimir-Polder force in levitation distances between $\sim 0.53 - 0.6\mu\text{m}$. All these results can be extended to Au and Si nanoparticles. In Sect.IVB of the Suppl. Mat. we show that levitation for SiC, Au and Si nanoparticles are possible between the 0.4-0.7 μm for the full-bandwidth PMC case.

By opposing the Casimir-Polder force and the nanoparticle's weight, the mechanical equilibrium position z_0 is given by $F_z(z_0) = mg$. As it was shown, we have $R \ll z_0 \approx 0.6\mu\text{m}$ irrespective of the temperatures, and in agreement to the point-dipole approximation. Furthermore, as for small nanoparticles the radiation reaction correction entering the force through the polarizability is negligible, z_0 results independent of the volume V . Thus, the levitation of nanoparticles interacting with a PMC surface shows to be feasible. The total potential perceived by the nanoparticle is calculated from the combination of the Casimir-Polder force with the weight as $U(z) = -\int_z^{+\infty} F_z(z')dz' + mgz$, which minimum corresponds to z_0 . This is shown in Fig.3.a as the blue

solid curve. Given the potential shape, levitation within a maximum and minimum distances is ensured. As the potential is not symmetric around z_0 , the motion on the z direction is, in general, anharmonic. As long as the nanoparticle's motion is limited to distances below $1\mu\text{m}$, thermal effects do not take a role. This is the case for an energy level $E(z_{\text{in}}) = U(z_{\text{in}})$, defined by the initial conditions $\{z(t_{\text{in}}) = z_{\text{in}}, \dot{z}(t_{\text{in}}) = 0\}$ (orange solid curve corresponding to $z_{\text{in}} = 0.42\mu\text{m}$). The actual motion of the nanoparticle is obtained from the equation of motion $m\ddot{z}(t) = F_z(z(t)) - mg$, subjected to the initial conditions. The anharmonic trajectory of the nanoparticle is shown in Fig.3.b, presenting a period $\sim 1\text{ms}$. Furthermore, for energy levels $E(\sim z_0)$, close to the potential minimum, the motion is harmonic, as shown by the orange dashed curves (taking $z_{\text{in}} = 0.57\mu\text{m} \approx z_0$). Then, the potential verifies $U(z) \approx m\Omega^2(z - z_0)^2/2$ (blue dotted curve), while the equation of motion is $\delta\ddot{z}(t) = -\Omega^2\delta z$, provided $\delta z \equiv z - z_0 \ll z_0$. The characteristic frequency is given by $\Omega \equiv [-(1/m)(dF_z/dz)|_{z_0}]^{1/2}$. According to Eq.(13), in the short-distance regime the force depends linearly on \hbar as an evidence of its quantum nature, so the frequency results:

$$\Omega^2 \approx \frac{5g}{z_0} = \frac{45\hbar c}{8\pi^2 \rho z_0^6} \frac{(\varepsilon_\infty - 1)}{(\varepsilon_\infty + 2)}, \quad (15)$$

which, as z_0 , is independent of V . For a SiC nanoparticle, $\Omega \approx 9013 \text{ s}^{-1}$ (or equivalently, $\nu = \Omega/[2\pi] \approx 1.4 \text{ KHz}$), giving a period of 0.7ms. Remarkably, while the first expression for the frequency Ω is minimal, the second one is linear on \hbar .

All in all, in this Letter we have analyzed the possibility of nanoparticle levitation by exploiting the Casimir-Polder force in combination with a novel PMC metamaterial design. We demonstrate an effective realistic design of a metamaterial with a broadband PMC property based on a multilayer configuration, although other equivalent options could also be explored [38]. We show that the Casimir-Polder force perceived by the nanoparticle is able to compensate its weight, ensuring levitation. This was shown for SiC, Au and Si nanoparticles. Having the nanoparticle's motion confined on the short-distances regime $z < 1\mu\text{m}$, the mechanism is sustained by the (quantum) zero-temperature contribution. Thus, the mechanism shows to be robust to thermal effects and feasible for experiments in vacuum. We finally show that quantum effects on the harmonic dynamics (around the equilibrium point z_0) gives a characteristic frequency with a linear dependence on Planck's constant \hbar and independent of the nanoparticle's volume V . Our work opens the way on the experimental and technological sides for nanoparticles levitation in vacuum with a minimalistic methodology and requirements, and also for achieving levitation of larger objects as parallel plates in frictionless contact.

V.G. acknowledges the Spanish Ministerio de Econo-

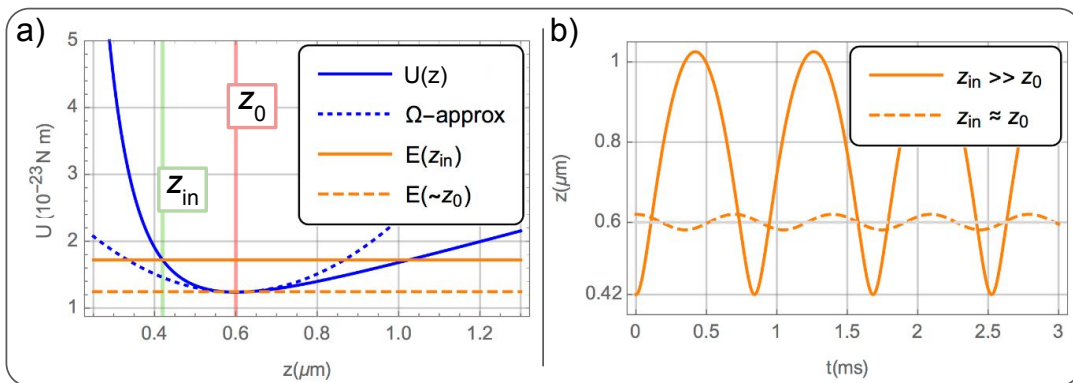


FIG. 3. Levitation for a SiC nanoparticle with $R = 50\text{nm}$ radius because of the interaction with a PMC plane surface, occurring at the mechanical equilibrium position $z_0 \approx 0.6\mu\text{m}$. Panel a) corresponds to the short-distance total potential U perceived by the nanoparticle from the combination between its weight and the Casimir-Polder force exerted by the PMC plane surface (blue solid curve). The dotted blue curve corresponds to the harmonic approximation of the potential around z_0 (vertical red line). The orange solid line corresponds to an energy of the nanoparticle associated to an initial position z_{in} (vertical green line) and zero initial velocity. The orange dashed line to an energy close to the potential minimum. Panel b) shows the resulting trajectories of the nanoparticle $z(t)$ for each energy level mentioned before. While the general motion is anharmonic, the low energies remains harmonic.

mia y Competitividad for financial support through the grant NANOTOPO (FIS2017-91413-EXP) and also the Ministerio de Ciencia, Innovación y Universidades through the grant MELODIA (PGC2018-095777-B-C21). V.G. thank the “ENSEMBLE3 - Centre of Excellence for nanophotonics, advanced materials and novel crystal growth-based technologies” project (GA No. MAB/2020/14) carried out within the International Research Agendas programme of the Foundation for Polish Science co-financed by the European Union under the European Regional Development Fund and the European Union’s Horizon 2020 research and innovation programme Teaming for Excellence (GA. No. 857543) for support of this work. We also thank Xiaofei Xiao for comments and suggestions on the manuscript.

* adrianrubiolopez0102@gmail.com

† <http://www.GianniniLab.com>

- [1] J. Gieseler, R. Quidant, C. Dellago, and L. Novotny, Dynamic relaxation of a levitated nanoparticle from a non-equilibrium steady state, *Nature Nanotechnology* **9**, 358 (2014), arXiv:1404.0411 [cond-mat.stat-mech].
- [2] A. Geraci, Levitating the fridge, *Nature Photonics* **11**, 613 (2017).
- [3] A. Manjavacas, F. J. Rodríguez-Fortuño, F. J. García de Abajo, and A. V. Zayats, Lateral casimir force on a rotating particle near a planar surface, *Phys. Rev. Lett.* **118**, 133605 (2017).
- [4] G. Winstone, R. Bennett, M. Rademacher, M. Rashid, S. Buhmann, and H. Ulbricht, Direct measurement of the electrostatic image force of a levitated charged nanoparticle close to a surface, *Phys. Rev. A* **98**, 053831 (2018).
- [5] D. C. Moore and A. A. Geraci, Searching for new physics using optically levitated sensors, arXiv e-prints , arXiv:2008.13197 (2020), arXiv:2008.13197 [quant-ph].
- [6] L. Martinetz, K. Hornberger, J. Millen, M. S. Kim, and B. A. Stickler, Quantum electromechanics with levitated nanoparticles, *npj Quantum Information* **6**, 101 (2020), arXiv:2005.14006 [quant-ph].
- [7] R. Ali, F. A. Pinheiro, R. S. Dutra, F. S. S. Rosa, and P. A. M. Neto, Probing the optical chiral response of single nanoparticles with optical tweezers, *J. Opt. Soc. Am. B* **37**, 2796 (2020).
- [8] F. Ricci, M. T. Cuairan, A. W. Schell, E. Hebestreit, R. A. Rica, N. Meyer, and R. Quidant, A chemical nano-reactor based on a levitated nanoparticle in vacuum, arXiv e-prints , arXiv:2107.01084 (2021), arXiv:2107.01084 [physics.chem-ph].
- [9] T. H. Boyer, Van der waals forces and zero-point energy for dielectric and permeable materials, *Physical Review A* **9**, 2078 (1974).
- [10] O. Kenneth, I. Klich, A. Mann, and M. Revzen, Repulsive casimir forces, *Physical review letters* **89**, 033001 (2002).
- [11] C. Henkel and K. Joulain, Casimir force between designed materials: What is possible and what not, *EPL (Europhysics Letters)* **72**, 929 (2005).
- [12] M. Levin, A. P. McCauley, A. W. Rodriguez, M. H. Reid, and S. G. Johnson, Casimir repulsion between metallic objects in vacuum, *Physical review letters* **105**, 090403 (2010).
- [13] K. A. Milton, E. Abalo, P. Parashar, N. Pourtolami, I. Brevik, and S. Å. Ellingsen, Repulsive casimir and casimir-polder forces, *Journal of Physics A: Mathematical and Theoretical* **45**, 374006 (2012).
- [14] K. Sinha, Repulsive vacuum-induced forces on a magnetic particle, *Physical Review A* **97**, 032513 (2018).
- [15] Q.-D. Jiang and F. Wilczek, Chiral casimir forces: Repulsive, enhanced, tunable, *Physical Review B* **99**, 125403 (2019).
- [16] J. J. Marchetta, P. Parashar, and K. Shajesh, Geometrical dependence in casimir-polder repulsion, *Physical Re-*

- view A **104**, 032209 (2021).
- [17] D. Iannuzzi and F. Capasso, Comment on “repulsive casimir forces”, *Physical Review Letters* **91**, 029101 (2003).
- [18] O. Kenneth and I. Klich, Opposites attract: A theorem about the casimir force, *Physical review letters* **97**, 160401 (2006).
- [19] F. S. Rosa, D. A. Dalvit, and P. W. Milonni, Casimir-lifshitz theory and metamaterials, *Physical Review Letters* **100**, 1 (2008).
- [20] F. Rosa, On the possibility of casimir repulsion using metamaterials, in *Journal of Physics: Conference Series*, Vol. 161 (IOP Publishing, 2009) p. 012039.
- [21] S. J. Rahi, M. Kardar, and T. Emig, Constraints on stable equilibria with fluctuation-induced (casimir) forces, *Physical review letters* **105**, 070404 (2010).
- [22] A. W. Rodriguez, A. P. McCauley, D. Woolf, F. Capasso, J. D. Joannopoulos, and S. G. Johnson, Nontouching Nanoparticle Diclusters Bound by Repulsive and Attractive Casimir Forces, *Phys. Rev. Lett.* **104**, 160402 (2010), arXiv:0912.2243 [quant-ph].
- [23] V. Estesó, S. Carretero-Palacios, and H. Míguez, Nanolevitation phenomena in real plane-parallel systems due to the balance between casimir and gravity forces, *The Journal of Physical Chemistry C* **119**, 5663 (2015).
- [24] R. Zhao, L. Li, S. Yang, W. Bao, Y. Xia, P. Ashby, Y. Wang, and X. Zhang, Stable Casimir equilibria and quantum trapping, *Science* **364**, 984 (2019).
- [25] S. J. Palmer, X. Xiao, N. Pazos-Perez, M. A. Correa-Duarte, S. A. Maier, R. V. Craster, R. A. Alvarez-Puebla, and V. Giannini, Extraordinarily transparent compact metallic metamaterials, *Nature Communications* , 2118 (2019).
- [26] X. Xiao, M. Turino, I. B. Becerril-Castro, S. A. Maier, R. A. Alvarez-Puebla, and V. Giannini, Extraordinarily transparent metaldielectrics for infrared and terahertz applications, *Advanced Photonics Research* , 2200190 (2022).
- [27] M. Born and E. Wolf, *Principles of optics: electromagnetic theory of propagation, interference and diffraction of light* (Elsevier, 2013).
- [28] V. Agranovich and V. Kravtsov, Notes on crystal optics of superlattices, *Solid State Communications* **55**, 85 (1985).
- [29] A. Poddubny, I. Iorsh, P. Belov, and Y. Kivshar, Hyperbolic metamaterials, *Nature photonics* **7**, 948 (2013).
- [30] J. J. Saarinen and J. Sipe, A green function approach to surface optics in anisotropic media, *Journal of Modern Optics* **55**, 13 (2008).
- [31] S. Torquato, *Random Heterogeneous Materials: Microstructure and Macroscopic Properties* (2002).
- [32] D. Stroud, The effective medium approximations: Some recent developments, *Superlattices and microstructures* **23**, 567 (1998).
- [33] G. W. Milton, *Correlation of the electromagnetic and elastic properties of composites and microgeometries corresponding with effective medium approximations* (1984).
- [34] M. G.W., The coherent potential approximation is a realizable effective medium scheme, *Comm. Math. Phys.* **99**, 463 (1985).
- [35] M. Hövel, B. Gompf, and M. Dressel, Dielectric properties of ultrathin metal films around the percolation threshold, *Physical Review B* **81**, 035402 (2010).
- [36] C. Henkel, K. Joulain, J. P. Mulet, and J. J. Greffet, Radiation forces on small particles in thermal near fields, *Journal of Optics A: Pure and Applied Optics* **4** (2002).
- [37] M. Antezza, L. P. Pitaevskii, and S. Stringari, New asymptotic behavior of the surface-atom force out of thermal equilibrium, *Physical Review Letters* **95**, 1 (2005).
- [38] A. K. Boddeti, A. Alabassi, V. Aggarwal, and Z. Jacob, Spectral domain inverse design for accelerating nanocomposite metamaterials discovery, *Opt. Mater. Express* **9**, 4765 (2019).

Casimir nanoparticle levitation in vacuum with broadband perfect magnetic conductor metamaterials

Adrián E. Rubio López^{1,*} and Vincenzo Giannini^{2,3,4}

¹*Birck Nanotechnology Center, School of Electrical and Computer Engineering,
Purdue University, West Lafayette, IN 47907, USA*

²*Technology Innovation Institute, P.O. Box 9639,
Building B04C, Masdar City, Abu Dhabi, United Arab Emirates*

³*Instituto de Estructura de la Materia (IEM-CSIC),*

Consejo Superior de Investigaciones Científicas, Serrano 121, 28006 Madrid, Spain

⁴*Centre of Excellence ENSEMBLE3 sp. z o.o., Wolczynska 133, Warsaw, 01-919, Poland[†]*

I. REFLECTION FROM A STRATIFIED MEDIUM MADE OF THIN FILMS

Here we review the governing reflection coefficients equations of a thin film stratified medium (see Fig. 1), we will follow the nomenclature and approach of Born and Wolf book (first chapter), Principle of Optics.

We will use the transfer matrix formalism to describe the reflection coefficients of systems as the one shown in Fig. 1, where without loss of generality, we are considering repeated pairs of thin layers.

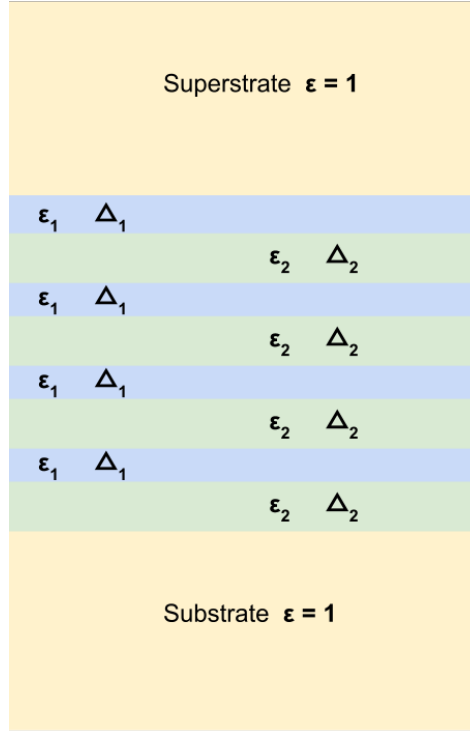


FIG. 1: Scheme of a multilayer made of thin films pairs with permittivities ϵ_1 and ϵ_2 and, thickness Δ_1 and Δ_2 . As superstrate and substrate we consider for simplicity we consider vacuum.

More in detail, for normal incidence light the characteristic matrix, \mathbf{M} , reads:

$$\mathbf{M} = \begin{bmatrix} 1 & -ik_0 B \\ -ik_0 A & 1 \end{bmatrix}, \quad (\text{S.1})$$

where

$$A = \sum_{n=1}^N \epsilon_n \Delta_n; \quad (\text{S.2})$$

$$B = \sum_{n=1}^N \mu_n \Delta_n, \quad (\text{S.3})$$

where $k = 2\pi/\lambda$ and, ε_n and μ_n are the relative permittivity and permeability of the n -th layer. Let's also assume that $\Delta_1 = \Delta_2 = \Delta$ and that $\mu = 1$,

$$A = \Delta \sum_{n=1}^N \varepsilon_n; \quad (\text{S.4})$$

$$B = L, \quad (\text{S.5})$$

where $\sum_n \Delta_n = L$ is the total thickness of the N layers. From the elements m_{ij} of the characteristics matrix \mathbf{M} , we can write the Fresnel reflections coefficients at normal incidence (see Born and Wolf), and, in particular r_s :

$$r_s = \frac{(m_{11} + m_{12}) - (m_{21} + m_{22})}{(m_{11} + m_{12}) + (m_{21} + m_{22})} = \frac{ik(A - L)}{2 - ik(A + L)}. \quad (\text{S.6})$$

If we chose the permittivity of the layers in a such way that $A = 0$, and $kL \gg 1$ we obtain

$$r_s = \frac{-ikL}{2 - ikL} \approx +1. \quad (\text{S.7})$$

II. CASIMIR-POLDER FORCE ON A NANOPARTICLE

Our general scenario of interest consists in a nanoparticle close to a surface in a out of thermal equilibrium situation, meaning that the nanoparticle, the surface and the enviromental EM field have different temperatures (T_{NP} , T_{S} and T_{EM} respectively). As the nanoparticle is considered to be of a typical size smaller than the typical wavelength of the surrounding radiation (with energies in the orders of $T_{\text{S,EM}}$, considering $k_{\text{B}} \equiv 1$), the nanoparticle interacts with the EM field through its dipole moment \mathbf{d} .

Therefore, following Ref.¹, the force over the dipole reads:

$$\mathbf{F}(\mathbf{r}) = \left\langle \hat{d}_i^{(\text{ind})}(t) \nabla \hat{E}_i^{(\text{fl})}(\mathbf{r}, t) \right\rangle + \left\langle \hat{d}_i^{(\text{fl})}(t) \nabla \hat{E}_i^{(\text{ind})}(\mathbf{r}, t) \right\rangle, \quad (\text{S.8})$$

where \mathbf{r} stands for the nanoparticle's position.

The first term describes the fluctuations of the field that correlate with the corresponding induced dipole, while the second involves dipole fluctuations and the field they induce. Crossed terms do not appear since there are no crossed correlations between the dipole and the field, since they originate from different physical systems.

On one hand, the dipole induced by the field fluctuations is given by the particle's polarizability $\alpha(\omega)$:

$$\hat{\mathbf{d}}^{(\text{ind})}(\omega) = \varepsilon_0 \alpha(\omega) \hat{\mathbf{E}}(\omega, \mathbf{r}), \quad (\text{S.9})$$

where $\hat{\mathbf{E}}(\omega, \mathbf{r})$ is the total electric field at the dipole's position. Working at lowest order in the polarizability, we can ignore the field scattered by the nanoparticle and replace it with $\hat{\mathbf{E}}^{(\text{fl})}(\omega, \mathbf{r})$. Otherwise, we could work with a 'dressed' polarizability.

On the other hand, the field induced by the dipole fluctuations is written in terms of the EM Green tensor:

$$\hat{\mathbf{E}}^{(\text{ind})}(\omega, \mathbf{x}) = \mathbf{G}(\omega, \mathbf{x}, \mathbf{r}) \cdot \hat{\mathbf{d}}(\omega), \quad (\text{S.10})$$

having that \mathbf{x} is an observation point. In analogy as before, to the lowest order, we can identify the total dipole with its fluctuating component $\hat{\mathbf{d}}^{(\text{fl})}$.

Moreover, by considering that:

$$\left\langle \hat{A}(t) \hat{B}(t) \right\rangle = \int \frac{d\omega}{2\pi} \frac{d\omega'}{2\pi} e^{i(\omega' - \omega)t} \left\langle \hat{A}(\omega) \hat{B}^\dagger(\omega') \right\rangle, \quad (\text{S.11})$$

we can proceed to write each term of the force given in Eq.(S.8). For these calculations, we require the correlations of the fluctuating dipole and of the different contributions of the field.

For the dipole fluctuations we appeal to the fluctuation-dissipation theorem which, assuming the nanoparticle to be at temperature T_{NP} , gives:

$$\left\langle \hat{\mathbf{d}}^{(\text{fl})}(\omega) \left[\hat{\mathbf{d}}^{(\text{fl})}(\omega') \right]^\dagger \right\rangle = 2\pi \delta(\omega - \omega') \delta_{ij} \frac{2\hbar \varepsilon_0}{(1 - e^{-\hbar\omega/(k_{\text{B}} T_{\text{NP}})})} \text{Im} [\alpha(\omega)]. \quad (\text{S.12})$$

It is important to notice that this expression applies for positive and negative frequencies. For $\omega > 0$, we have $(1 - \text{Exp}[-\hbar\omega/(k_B T_i)])^{-1} = 1 + \bar{n}_i(\omega)$, with $\bar{n}_i(\omega)$ the Bose-Einstein occupation number at temperature T_i . For $\omega < 0$, we have $(1 - \text{Exp}[-\hbar\omega/(k_B T_i)])^{-1} = -\bar{n}_i(|\omega|)$. The minus sign is compensated by the oddness of the imaginary part of the polarizability. In our notation, we will keep present in the subscripts the value of the temperatures T_i at \bar{n}_i in order to avoid any confusion since we are dealing with nonequilibrium situations involving multiple temperatures.

Therefore, we can prove that for the dipole fluctuations term we have:

$$\begin{aligned} \left\langle \hat{d}_i^{(\text{fl})}(t) \nabla \hat{E}_i^{(\text{ind})}(\mathbf{r}, t) \right\rangle &= 2\hbar\varepsilon_0 \int_{-\infty}^{+\infty} \frac{d\omega}{2\pi} \frac{\text{Im}[\alpha(\omega)]}{(1 - e^{-\hbar\omega/(k_B T_{\text{NP}})})} \nabla [G_{ii}^*(\omega, \mathbf{r}, \mathbf{r}')] \Big|_{\mathbf{r}'=\mathbf{r}} \\ &= 2\hbar\varepsilon_0 \int_0^{+\infty} \frac{d\omega}{2\pi} \text{Im}[\alpha(\omega)] (\nabla [G_{ii}^*(\omega, \mathbf{r}, \mathbf{r}')] \Big|_{\mathbf{r}'=\mathbf{r}} + 2\bar{n}_{\text{NP}}(\omega) \text{Re}[\nabla [G_{ii}(\omega, \mathbf{r}, \mathbf{r}')] \Big|_{\mathbf{r}'=\mathbf{r}}]), \end{aligned} \quad (\text{S.13})$$

where we have considered $\coth[\hbar\omega/(2k_B T_i)] = 1 + 2\bar{n}_i(\omega)$ as $\omega > 0$.

Furthermore, in our particular case of a half-space, as the source and observation point are equal to the position of the dipole (\mathbf{r}) in free space, the EM Green tensor will be constituted by two parts: $G_{ij}(\omega, \mathbf{r}, \mathbf{r}') = G_{ij}^{(\text{Free})}(\omega, \mathbf{r}, \mathbf{r}') + G_{ij}^{(\text{Refl})}(\omega, \mathbf{r}, \mathbf{r}')$, where the first term correspond to the free field Green tensor and the second one to the reflection from the half-space. However, it can be checked that, under the derivative, the free field part vanishes when setting $\mathbf{r}' = \mathbf{r}$ due to isotropy (which means that $G_{ij}^{(\text{Free})}(\omega, \mathbf{r}, \mathbf{r}') = G_{ij}^{(\text{Free})}(\omega, \mathbf{r} - \mathbf{r}')$) and thus we have that $\nabla [G_{ij}(\omega, \mathbf{r}, \mathbf{r}')] \Big|_{\mathbf{r}'=\mathbf{r}} = \nabla [G_{ij}^{(\text{Refl})}(\omega, \mathbf{r}, \mathbf{r}')] \Big|_{\mathbf{r}'=\mathbf{r}}$.

On the other hand, for the field fluctuations' contribution, we can write:

$$\left\langle \hat{d}_i^{(\text{ind})}(t) \nabla \hat{E}_i^{(\text{fl})}(\mathbf{r}, t) \right\rangle = \int \frac{d\omega}{2\pi} \frac{d\omega'}{2\pi} e^{i(\omega' - \omega)t} \varepsilon_0 \alpha(\omega) \delta_{ij} \nabla' \left[\left\langle \hat{E}_i^{(\text{fl})}(\omega, \mathbf{r}) \left[\hat{E}_j^{(\text{fl})}(\omega', \mathbf{r}') \right]^\dagger \right\rangle \right] \Big|_{\mathbf{r}'=\mathbf{r}}. \quad (\text{S.14})$$

Thus, the correlations of the electric field are required, i.e., the field fluctuations. These have two contributions: one coming from the thermal currents in the material half-space, and a second one coming from the field fluctuations in the empty half-space:

$$\left\langle \hat{E}_i^{(\text{fl})}(\omega, \mathbf{r}) \left[\hat{E}_j^{(\text{fl})}(\omega', \mathbf{r}') \right]^\dagger \right\rangle = 2\pi\delta(\omega - \omega') [W_{ij}(\omega, T_S, \mathbf{r}, \mathbf{r}') + V_{ij}(\omega, T_{\text{EM}}, \mathbf{r}, \mathbf{r}')]. \quad (\text{S.15})$$

At this point, it is worth noting that each contribution (W_{ij}, V_{ij}) can be splitted as a sum of a zero-point fluctuation plus a thermal contribution in the following way:

$$W_{ij}(\omega, T_S, \mathbf{r}, \mathbf{r}') = \{\theta(\omega) [1 + \bar{n}_S(\omega)] - \theta(-\omega)\bar{n}_S(|\omega|)\} W_{ij}(\omega, \mathbf{r}, \mathbf{r}'), \quad (\text{S.16})$$

$$V_{ij}(\omega, T_{\text{EM}}, \mathbf{r}, \mathbf{r}') = \{\theta(\omega) [1 + \bar{n}_{\text{EM}}(\omega)] - \theta(-\omega)\bar{n}_{\text{EM}}(|\omega|)\} V_{ij}(\omega, \mathbf{r}, \mathbf{r}'), \quad (\text{S.17})$$

where the second terms vanish for the corresponding zero temperature limit ($T_S, T_{\text{EM}} \rightarrow 0$).

At the same time, the first two terms combine to give the zero-temperature fluctuation-dissipation theorem:

$$W_{ij}(\omega, 0, \mathbf{r}, \mathbf{r}') + V_{ij}(\omega, 0, \mathbf{r}, \mathbf{r}') = 2\hbar\theta(\omega) \text{Im} [G_{ij}(\omega, \mathbf{r}, \mathbf{r}')], \quad (\text{S.18})$$

where the Heaviside function from the limit:

$$\theta(\omega) = \lim_{T \rightarrow 0} \frac{1}{1 - e^{-\hbar\omega/(k_B T)}}. \quad (\text{S.19})$$

Equivalently for $W_{ij}(\omega, \mathbf{r}, \mathbf{r}')$, $V_{ij}(\omega, \mathbf{r}, \mathbf{r}')$, we can write:

$$W_{ij}(\omega, \mathbf{r}, \mathbf{r}') + V_{ij}(\omega, \mathbf{r}, \mathbf{r}') = 2\hbar \text{Im} [G_{ij}(\omega, \mathbf{r}, \mathbf{r}')], \quad (\text{S.20})$$

Thus, we have:

$$V_{ij}(\omega, T_{\text{EM}}, \mathbf{r}, \mathbf{r}') = \{\theta(\omega) [1 + \bar{n}_{\text{EM}}(\omega)] - \theta(-\omega)\bar{n}_{\text{EM}}(|\omega|)\} [2\hbar \text{Im} [G_{ij}(\omega, \mathbf{r}, \mathbf{r}')] - W_{ij}(\omega, \mathbf{r}, \mathbf{r}')], \quad (\text{S.21})$$

Now, following Ref.¹, from Lifshitz theory, considering that the radiation generated by the material half-space is due to fluctuating sources playing the role of a polarization field, and assuming local thermal equilibrium, we use the fluctuation-dissipation theorem to calculate the contribution of the material plane to the field fluctuations, obtaining:

$$W_{ij}(\omega, T_S, \mathbf{r}, \mathbf{r}') = 2\hbar\varepsilon_0 \frac{\text{Im}[\varepsilon_S(\omega)]}{(1 - e^{-\hbar\omega/(k_B T_S)})} S_{ij}(\omega, \mathbf{r}, \mathbf{r}'), \quad (\text{S.22})$$

with $\varepsilon_S(\omega)$ the permittivity of the material half-space and:

$$S_{ij}(\omega, \mathbf{r}, \mathbf{r}') = \int_{V_S} d\mathbf{x} G_{ik}(\omega, \mathbf{r}, \mathbf{x}) G_{jk}^*(\omega, \mathbf{r}', \mathbf{x}). \quad (\text{S.23})$$

This allow us to prove the fundamental property of the functions W_{ij}, V_{ij} :

$$W_{ij}(-\omega, \mathbf{r}, \mathbf{r}') = -W_{ij}^*(\omega, \mathbf{r}, \mathbf{r}') \quad , \quad V_{ij}(-\omega, \mathbf{r}, \mathbf{r}') = -V_{ij}^*(\omega, \mathbf{r}, \mathbf{r}'), \quad (\text{S.24})$$

provided also that $G_{ij}(-\omega, \mathbf{r}, \mathbf{r}') = G_{ij}^*(\omega, \mathbf{r}, \mathbf{r}')$.

The electric field correlation reads:

$$\begin{aligned} \left\langle \hat{E}_i^{(\text{fl})}(\omega, \mathbf{r}) \left[\hat{E}_j^{(\text{fl})}(\omega', \mathbf{r}') \right]^\dagger \right\rangle &= 2\pi\delta(\omega - \omega') \left(2\hbar [\theta(\omega) (1 + \bar{n}_{\text{EM}}(\omega)) - \theta(-\omega)\bar{n}_{\text{EM}}(|\omega|)] \text{Im} [G_{ij}(\omega, \mathbf{r}, \mathbf{r}')] \right. \\ &\quad \left. + \{ \theta(\omega) [\bar{n}_S(\omega) - \bar{n}_{\text{EM}}(\omega)] - \theta(-\omega) [\bar{n}_S(|\omega|) - \bar{n}_{\text{EM}}(|\omega|)] \} W_{ij}(\omega, \mathbf{r}, \mathbf{r}') \right). \end{aligned} \quad (\text{S.25})$$

The contribution to the force then reads:

$$\begin{aligned} \left\langle \hat{d}_i^{(\text{ind})}(t) \nabla \hat{E}_i^{(\text{fl})}(\mathbf{r}, t) \right\rangle &= 2\varepsilon_0 \int_0^{+\infty} \frac{d\omega}{2\pi} \left[\hbar [\alpha(\omega) + 2\text{Re}[\alpha(\omega)] \bar{n}_{\text{EM}}(\omega)] \text{Im} [\nabla [G_{ii}(\omega, \mathbf{r}, \mathbf{r}')] |_{\mathbf{r}'=\mathbf{r}}] \right. \\ &\quad \left. + [\bar{n}_S(\omega) - \bar{n}_{\text{EM}}(\omega)] \text{Re} [\alpha(\omega) \nabla' [W_{ii}(\omega, \mathbf{r}, \mathbf{r}')] |_{\mathbf{r}'=\mathbf{r}}] \right], \end{aligned} \quad (\text{S.26})$$

where we have used that $\nabla [G_{ii}(\omega, \mathbf{r}, \mathbf{r}')] |_{\mathbf{r}'=\mathbf{r}} = \nabla' [G_{ii}(\omega, \mathbf{r}, \mathbf{r}')] |_{\mathbf{r}'=\mathbf{r}}$.

Considering this last equation, we can write the force over the dipole as:

$$\begin{aligned} \mathbf{F}(\mathbf{r}) &= 2\varepsilon_0 \int_0^{+\infty} \frac{d\omega}{2\pi} \left[\hbar \coth \left(\frac{\hbar\omega}{2k_B T_{\text{EM}}} \right) \text{Re} [\alpha(\omega)] \text{Im} [\nabla [G_{ii}(\omega, \mathbf{r}, \mathbf{r}')] |_{\mathbf{r}'=\mathbf{r}}] \right. \\ &\quad \left. + \hbar \coth \left(\frac{\hbar\omega}{2k_B T_{\text{NP}}} \right) \text{Im} [\alpha(\omega)] \text{Re} [\nabla [G_{ii}(\omega, \mathbf{r}, \mathbf{r}')] |_{\mathbf{r}'=\mathbf{r}}] + [\bar{n}_S(\omega) - \bar{n}_{\text{EM}}(\omega)] \text{Re} [\alpha(\omega) \nabla' [W_{ii}(\omega, \mathbf{r}, \mathbf{r}')] |_{\mathbf{r}'=\mathbf{r}}] \right], \end{aligned} \quad (\text{S.27})$$

where the force results to be explicitly real.

Now, we have to evaluate the EM Green tensor and the function W_{ij} for our particular case. Following Ref.¹, for the case of a half-space with surface at $z = 0$, the reflection part of the EM Green tensor is given by:

$$G_{ij}^{(\text{Refl})}(\omega, \mathbf{r}, \mathbf{r}') = \int \frac{d^2 K}{(2\pi)^2} e^{i\mathbf{K} \cdot (\mathbf{R} - \mathbf{R}')} e^{i\gamma(z+z')} g_{ij}(\omega, \mathbf{K}), \quad (\text{S.28})$$

with:

$$g_{ij}(\omega, \mathbf{K}) = \frac{i\omega^2}{2\varepsilon_0 c^2 \gamma} \sum_{\mu=s,p} e_{\mu,i}^{(r)} e_{\mu,j}^{(i)} r_\mu, \quad (\text{S.29})$$

where $\mathbf{K} = (k_x, k_y, 0)$ and $\gamma = \sqrt{\omega^2/c^2 - K^2}$ is the wavevector component perpendicular to the interface. The unit vectors $\mathbf{e}_\mu^{(i,r)}$ describe the polarization of plane waves incident from the vacuum half-space $z > 0$ and reflected from the interface, respectively, with reflection coefficient r_μ . The polarization vectors are given by $\mathbf{e}_s^{(i,r)} = \hat{\mathbf{K}} \times \mathbf{e}_z$, $\mathbf{e}_p^{(i)} = (K\mathbf{e}_z + \gamma\hat{\mathbf{K}})c/\omega$, and $\mathbf{e}_p^{(r)} = (K\mathbf{e}_z - \gamma\hat{\mathbf{K}})c/\omega$, where $\hat{\mathbf{K}} = \mathbf{K}/K$ is a unit vector.

On the other hand, the function W_{ij} is given by:

$$W_{ij}(\omega, T, \mathbf{r}, \mathbf{r}') = \frac{2\hbar\omega^3}{3\pi\varepsilon_0 c^3 \left(1 - e^{-\frac{\hbar\omega}{k_B T}}\right)} \int \frac{d^2 K}{(2\pi)^2} e^{i\mathbf{K} \cdot (\mathbf{R} - \mathbf{R}')} e^{i(\gamma z - \gamma^* z')} \mathbb{W}_{ij}(\omega, \mathbf{K}) \equiv \frac{1}{\left(1 - e^{-\frac{\hbar\omega}{k_B T}}\right)} W_{ij}(\omega, \mathbf{r}, \mathbf{r}'), \quad (\text{S.30})$$

with:

$$\mathbb{W}_{ij}(\omega, \mathbf{K}) = \frac{3\pi c \operatorname{Re}(\gamma_S)}{4\omega |\gamma_S|^2} \sum_{\mu=s,p} e_{\mu,i}^{(t)} e_{\mu,j}^{(t)*} |e_{\mu}^{(S)}|^2 |t_{\mu}|^2, \quad (\text{S.31})$$

where $\gamma_S = \sqrt{\varepsilon_S \omega^2 / c^2 - K^2}$ is the perpendicular wavevector component inside the substrate. The substrate and vacuum polarization vectors are denoted $\mathbf{e}_{\mu}^{(S,t)}$, respectively, with the transmission coefficient t_{μ} . The polarization vectors are given by $\mathbf{e}_{\mu}^{(t)} = \mathbf{e}_{\mu}^{(r)}$, $\mathbf{e}_s^{(S)} = \hat{\mathbf{K}} \times \mathbf{e}_z$ and $\mathbf{e}_p^{(S)} = (K\mathbf{e}_z - \gamma_S \hat{\mathbf{K}})c / \sqrt{\varepsilon_S} \omega$.

For the numerical integration, the integral over the angle \mathbf{K} is performed analytically. The radial K integral left in and the integrals over ω have to be performed numerically.

It is worth noting that $W_{ii}(\omega, T, \mathbf{r}, \mathbf{r})$ is real and positive.

Then, it is straightforward to prove that:

$$g_{ii}(\omega, \mathbf{K}) = \frac{i}{2\varepsilon_0 \gamma} \left[\frac{\omega^2}{c^2} r_s + (K^2 - \gamma^2) r_p \right] \equiv ig(\omega, K), \quad (\text{S.32})$$

$$\mathbb{W}_{ii}(\omega, \mathbf{K}) = \frac{3\pi c \operatorname{Re}(\gamma_S)}{4\omega |\gamma_S|^2} \left[|t_s|^2 + \frac{c^4}{|\varepsilon_S| \omega^4} (K^2 + |\gamma|^2) (K^2 + |\gamma_S|^2) |t_p|^2 \right] \equiv \mathbb{W}(\omega, K), \quad (\text{S.33})$$

having that $\mathbb{W}(\omega, K) > 0$ for every ω, K .

And therefore, by deriving, changing to polar coordinates and integrating the angular variable:

$$\nabla [G_{ii}(\omega, \mathbf{r}, \mathbf{r}')] |_{\mathbf{r}'=\mathbf{r}} = i\mathbf{e}_z \int_0^{+\infty} \frac{dK}{2\pi} K \gamma e^{i2\gamma z} ig(\omega, K), \quad (\text{S.34})$$

$$\nabla' [W_{ii}(\omega, \mathbf{r}, \mathbf{r}')] |_{\mathbf{r}'=\mathbf{r}} = -\frac{i2\hbar\omega^3}{3\pi\varepsilon_0 c^3} \mathbf{e}_z \int_0^{+\infty} \frac{dK}{2\pi} K \gamma^* e^{-2\operatorname{Im}(\gamma)z} \mathbb{W}(\omega, K). \quad (\text{S.35})$$

Finally, the force over the dipole results along the z -axis and only depending on z (the distance of the nanoparticle to the plate), $\mathbf{F}(\mathbf{r}) = \mathbf{e}_z F_z(z)$ reads:

$$\begin{aligned} F_z(z) = & 2\hbar\varepsilon_0 \int_0^{+\infty} \frac{d\omega}{2\pi} \int_0^{+\infty} \frac{dK}{2\pi} K \left[\coth \left[\frac{\hbar\omega}{2k_B T_{\text{EM}}} \right] \operatorname{Re}[\alpha(\omega)] \operatorname{Re}[\gamma e^{i2\gamma z} ig(\omega, K)] \right. \\ & - \coth \left[\frac{\hbar\omega}{2k_B T_{\text{NP}}} \right] \operatorname{Im}[\alpha(\omega)] \operatorname{Im}[\gamma e^{i2\gamma z} ig(\omega, K)] \\ & \left. + [\bar{n}_S(\omega) - \bar{n}_{\text{EM}}(\omega)] \frac{2\omega^3}{3\pi\varepsilon_0 c^3} [\operatorname{Im}[\alpha(\omega)] \operatorname{Re}(\gamma) - \operatorname{Re}[\alpha(\omega)] \operatorname{Im}(\gamma)] e^{-2\operatorname{Im}(\gamma)z} \mathbb{W}(\omega, K) \right]. \quad (\text{S.36}) \end{aligned}$$

At first sight, we can clearly differentiate the contributions due to the dispersive nature of the nanoparticle, which are all the terms including $\operatorname{Re}[\alpha(\omega)]$, and to the absorption of the nanoparticle, given by the terms including $\operatorname{Im}[\alpha(\omega)]$.

At the same time, we can eventually discriminate the contributions of the propagating and evanescent modes in vacuum. As $\gamma = \sqrt{\omega^2/c^2 - K^2}$, the modes having ω, K such that $\gamma = \operatorname{Re}(\gamma)$ are the propagating modes, while the modes such that $\gamma = i\operatorname{Im}(\gamma)$ are the evanescent modes. The second line in the last equation clearly presents the separation between them, where each set is correlated to the dispersion and absorption provided by the nanoparticle. In this term, the propagating modes are associated to the absorption of the nanoparticle while the evanescent ones are associated to the dispersion of the nanoparticle. On the other hand, in the first line, the modes are not correlated with a specific property of the nanoparticle.

Another separation that is implicit in the form that Eq.(S.36) is written relates to the Fresnel's coefficients associated to the plate. It is worth noting that, on one hand, g only depends on the reflection coefficients $r_{s,p}$, while \mathbb{W} depends on the transmission coefficients $t_{s,p}$. Thus, the first line of the r.h.s. of Eq.(S.36) only depends on $r_{s,p}$, while the second line on $t_{s,p}$.

To simplify the expression, we can recast it in the following way:

$$\begin{aligned} F_z(z) = & - \int_0^{+\infty} \frac{d\omega}{2\pi} \left[\coth \left[\frac{\hbar\omega}{2k_B T_{\text{EM}}} \right] \operatorname{Re}[\alpha(\omega)] \operatorname{Im}[\mathcal{R}(\omega, z)] + \coth \left[\frac{\hbar\omega}{2k_B T_{\text{NP}}} \right] \operatorname{Im}[\alpha(\omega)] \operatorname{Re}[\mathcal{R}(\omega, z)] \right. \\ & \left. + [\bar{n}_{\text{EM}}(\omega) - \bar{n}_S(\omega)] [\operatorname{Im}[\alpha(\omega)] \operatorname{Re}[\mathcal{T}(\omega, z)] - \operatorname{Re}[\alpha(\omega)] \operatorname{Im}[\mathcal{T}(\omega, z)]] \right], \quad (\text{S.37}) \end{aligned}$$

with:

$$\mathcal{R}(\omega, z) = 2\hbar\varepsilon_0 \int_0^{+\infty} \frac{dK}{2\pi} K\gamma e^{i2\gamma z} g(\omega, K) \quad , \quad \mathcal{T}(\omega, z) = \frac{4\hbar\omega^3}{3\pi c^3} \int_0^{+\infty} \frac{dK}{2\pi} K\gamma e^{-2\text{Im}(\gamma)z} \mathbb{W}(\omega, K). \quad (\text{S.38})$$

Notice that written in this way, \mathcal{R} only contains information on the reflection coefficients of the surface, while \mathcal{T} depends on the transmission ones. We can also notice that at zero temperature, only the first line of Eq.(S.37) contributes to the force. Thus, we can split this zero-point fluctuations contribution to obtain Eq.(10) of the manuscript:

$$F_z(z) = F_0(z) + F_R(z, T_{\text{EM}}, T_{\text{NP}}) + F_T(z, T_{\text{EM}}, T_S), \quad (\text{S.39})$$

with each contribution given by:

$$F_0(z) = -\text{Im} \left[\int_0^{+\infty} \frac{d\omega}{2\pi} \alpha(\omega) \mathcal{R}(\omega, z) \right], \quad (\text{S.40})$$

$$F_R(z, T_{\text{EM}}, T_{\text{NP}}) = -2 \int_0^{+\infty} \frac{d\omega}{2\pi} [\bar{n}_{\text{EM}}(\omega) \text{Re}[\alpha(\omega)] \text{Im}[\mathcal{R}(\omega, z)] + \bar{n}_{\text{NP}}(\omega) \text{Im}[\alpha(\omega)] \text{Re}[\mathcal{R}(\omega, z)]], \quad (\text{S.41})$$

$$F_T(z, T_{\text{EM}}, T_S) = - \int_0^{+\infty} \frac{d\omega}{2\pi} [\bar{n}_{\text{EM}}(\omega) - \bar{n}_S(\omega)] [\text{Im}[\alpha(\omega)] \text{Re}[\mathcal{T}(\omega, z)] - \text{Re}[\alpha(\omega)] \text{Im}[\mathcal{T}(\omega, z)]]. \quad (\text{S.42})$$

In general, the zero point contribution is obtained by means of Wick rotation on the complex ω -plane under some analytical conditions of the integrand on the first quadrant. Provided that $\alpha(i\omega) \in \mathbb{R}$ and $\mathcal{R}(i\omega, z) \in \mathbb{R}$, it is common to obtain:

$$F_0(z) = - \int_0^{+\infty} \frac{d\omega}{2\pi} \alpha(i\omega) \mathcal{R}(i\omega, z). \quad (\text{S.43})$$

This contribution depends only on the reflection coefficients of the surface, as it happens for the contribution F_R , while F_T depends exclusively on the surface's transmission coefficients. Moreover, notice that by considering a scenario where the plane surface and the surrounding EM field are characterized by a unique environmental temperature ($T_{\text{EM}} = T_S \equiv T_{\text{Env}}$) we have that $F_T(z, T_{\text{Env}}, T_{\text{Env}}) = 0$, which shows that the force in this scenario only depends on the reflection coefficients but not on the transmission.

III. THE CASIMIR-POLDER FORCE FOR A METAMATERIAL SURFACE AND THE PERFECT (ELECTRIC OR MAGNETIC) CONDUCTOR LIMIT

The expression for the force on Eq.(S.43) is completely general for describing the EM interaction of a dipolar point-object placed at a distance z from a material plate. As we mentioned before, the information about the nature of the plate is mainly encoded on the Fresnel's reflection and transmission coefficients $\{r_{s,p}; t_{s,p}\}$. The surface's material in our work is given by Eqs.(5-7) of the manuscript. As it mentioned, to a good level of approximation, we can write the reflection coefficients as:

$$r_s = \mp 1 - b\chi \quad , \quad r_p = \pm 1 \quad , \quad (\text{S.44})$$

with $b = 0, 1$ either the surface is a perfect conductor or the proposed metamaterial, respectively. The \mp signs stands for the PEC and PMC cases. Before Wick rotation, the kernel \mathcal{R} can be written as:

$$\mathcal{R}(\omega, z) = \pm \mathcal{R}_{\text{PC}}(\omega, z) + b\Delta\mathcal{R}(\omega, z), \quad (\text{S.45})$$

with:

$$\mathcal{R}_{\text{PC}}(\omega, z) = 2\hbar \int_0^{+\infty} \frac{dK}{2\pi} K e^{i2\gamma z} \gamma^2 \quad , \quad \Delta\mathcal{R}(\omega, z) = 2\hbar \int_0^{+\infty} \frac{dK}{2\pi} K e^{i2\gamma z} \left(i\sqrt{K^2 \left[\frac{\omega^2}{c^2} - K^2 \right]} + K^2 \right). \quad (\text{S.46})$$

Again, the two signs of the force are compatible with what it is intuitively expected from the interaction with image objects as described before.

For the full-bandwidth perfect conductors ($b = 0$), it is straightforward that the total force for the PEC and PMC cases relate each other as:

$$F_z^{(\text{PMC})} = -F_z^{(\text{PEC})}, \quad (\text{S.47})$$

which also applies at zero-temperature and the short-distances regime.

At this point, Wick rotation ($\omega \rightarrow i\omega$) can be introduced for calculating the two contributions of kernel \mathcal{R} , obtaining:

$$\mathcal{R}_{\text{PC}}(i\omega, z) = 2\hbar \int_0^{+\infty} \frac{dK}{2\pi} K e^{-2\sqrt{K^2 + \frac{\omega^2}{c^2}}z} \left(K^2 + \frac{\omega^2}{c^2} \right), \quad (\text{S.48})$$

$$\Delta\mathcal{R}(i\omega, z) = 2\hbar \int_0^{+\infty} \frac{dK}{2\pi} K e^{-2\sqrt{K^2 + \frac{\omega^2}{c^2}}z} \left(K^2 - \sqrt{K^2 \left[\frac{\omega^2}{c^2} + K^2 \right]} \right). \quad (\text{S.49})$$

By simple substitutions $K = (\omega/c)\sqrt{p^2 - 1}$, the integrals can be performed immediately:

$$\mathcal{R}_{\text{PC}}(i\omega, z) = \frac{\hbar \omega^4}{\pi c^4} \int_1^{+\infty} dp p^3 e^{-2\frac{\omega}{c}pz} = -\frac{3\hbar}{8\pi z^4} A(i\omega, z) e^{-2\frac{\omega}{c}z}, \quad (\text{S.50})$$

$$\begin{aligned} \Delta\mathcal{R}(i\omega, z) &= \frac{\hbar \omega^4}{\pi c^4} \int_1^{+\infty} dp p e^{-2\frac{\omega}{c}pz} \left(p^2 - 1 - p\sqrt{p^2 - 1} \right) \\ &= \frac{\hbar}{8\pi z^4} \left[e^{-2\frac{\omega}{c}z} \left(3 + 6\frac{\omega}{c}z + 4\frac{\omega^2}{c^2}z^2 \right) - 4\frac{\omega^3}{c^3}z^3 \mathcal{K}_1 \left(2\frac{\omega}{c}z \right) - 6\frac{\omega^2}{c^2}z^2 \mathcal{K}_2 \left(2\frac{\omega}{c}z \right) \right]. \end{aligned} \quad (\text{S.51})$$

with $A(i\omega, z) = \sum_{n=0}^3 \frac{1}{n!} \left(2\frac{\omega}{c}z \right)^n$ and \mathcal{K}_n the modified Bessel function of the second kind.

After this simplification, we can see that the distinction on the contributions of the TE and TM modes has disappeared. This aspect is related to the fact that for a PC, all the modes are totally reflected without distinction.

Now, we turn to the frequency integration. For this, we start commenting on the properties of the polarizability. For a nanoparticle made of a material of permittivity ε , the polarizability is given by the Clausius-Mossoti formula:

$$\alpha(\omega) = V\xi(\omega) = 3V \frac{[\varepsilon(\omega) - 1]}{[\varepsilon(\omega) + 2]}, \quad (\text{S.52})$$

where ξ corresponds to the polarizability per unit volume. In order to have a causal function $\alpha(t)$, the polarizability $\alpha(\omega)$ must have poles ($\{\nu_m\}$) lying on the lower-half of the complex plane (i.e., $\text{Im}[\nu_m] < 0 \forall m$). Notice that we are not considering poles of $\alpha(\omega)$ on the real axis. Furthermore, for the typical material models, it happens that $\alpha(i\omega) \in \mathbb{R} \forall \omega$.

At the short-distance regime (defined by $k_{\text{B}}Tz/[\hbar c] \ll 1$), the Casimir-Polder force between a point object and a plane surface is given by the zero-temperature contribution (see Ref.² and Sect.IVA below), which according to Eq.(S.43) is given by:

$$F_0(z) = \pm F_0^{(\text{PC})}(z) + b\Delta F_0(z). \quad (\text{S.53})$$

where \pm applies to the PMC and PEC cases respectively and having:

$$F_0^{(\text{PC})}(z) = \frac{3\hbar V}{8\pi z^4} \int_0^{+\infty} \frac{d\omega}{2\pi} \xi(i\omega) A(i\omega, z) e^{-2\frac{\omega}{c}z}, \quad (\text{S.54})$$

$$\Delta F_0(z) = \frac{3\hbar V}{8\pi z^4} \frac{1}{3} \int_0^{+\infty} \frac{d\omega}{2\pi} \xi(i\omega) \left[e^{-2\frac{\omega}{c}z} \left(3 + 6\frac{\omega}{c}z + 4\frac{\omega^2}{c^2}z^2 \right) - 4\frac{\omega^3}{c^3}z^3 \mathcal{K}_1 \left(2\frac{\omega}{c}z \right) - 6\frac{\omega^2}{c^2}z^2 \mathcal{K}_2 \left(2\frac{\omega}{c}z \right) \right]. \quad (\text{S.55})$$

Notice that for $b = 0$, we get $F_0 \rightarrow \pm F_0^{(\text{PC})}$ corresponding to the force by a full-bandwidth perfect conductor surface (PMC or PEC) as Eq.(12) of the manuscript. By taking the $+$ and $b = 1$ we obtain $F_0 \rightarrow F_0^{(\text{FM})} = F_0^{(\text{PC})} + \Delta F_0$ corresponding to the force by a metamaterial surface as mentioned on Eq.(14). On these two limiting cases we are not including the possibility of frequency cutoffs.

To go further, we consider a SiC nanoparticle of radius $R = 50\text{nm}$ in front of a full-bandwidth PMC surface. The permittivity model is $\varepsilon_{\text{SiC}}(\omega) = \varepsilon_\infty(\omega_L^2 - \omega^2 - i\gamma\omega)/(\omega_T^2 - \omega^2 - i\gamma\omega)$, where $\omega_L = 18.253 \times 10^{13}\text{s}^{-1}$, $\omega_T = 14.937 \times 10^{13}\text{s}^{-1}$, $\gamma = 8.966 \times 10^{11}\text{s}^{-1}$ and $\varepsilon_\infty = 6.7$. By a change of variables to the dimensionless variable $w = 2\omega z/c$ we show that:

$$F_0^{(\text{PC})}(z) = \frac{9\hbar cV}{32\pi^2 z^5} \frac{(\varepsilon_\infty - 1)}{(\varepsilon_\infty + 2)} \mathcal{I}(z), \quad (\text{S.56})$$

with:

$$\mathcal{I}(z) = \int_0^{+\infty} dw \frac{\left[w^2 + \frac{2\gamma}{c}zw + \left(\frac{2z}{c}\right)^2 \frac{(\varepsilon_\infty\omega_L^2 - \omega_T^2)}{(\varepsilon_\infty - 1)} \right]}{\left[w^2 + \frac{2\gamma}{c}zw + \left(\frac{2z}{c}\right)^2 \frac{(\varepsilon_\infty\omega_L^2 + 2\omega_T^2)}{(\varepsilon_\infty + 2)} \right]} \left(1 + w + \frac{w^2}{2} + \frac{w^3}{6} \right) e^{-w}. \quad (\text{S.57})$$

Now, it turns out that the integrand of $\mathcal{I}(z)$ decays approximately to 0 for $w > 20$ and any $0 < z < 1\mu\text{m}$. Moreover, within the same range of distances z , we have that $\mathcal{I}(z) \approx \mathcal{I}(0) = 4$ with a difference on the order of 3%. Then, we have to a good level of approximation that:

$$F_0^{(\text{PC})}(z) \approx \frac{9\hbar cV}{8\pi^2 z^5} \frac{(\varepsilon_\infty - 1)}{(\varepsilon_\infty + 2)}, \quad (\text{S.58})$$

which corresponds to the result shown in Eq.(13) of the manuscript.

Remarkably, the same expression is valid approximately (exactly) for Au (Si) by the replacement $\varepsilon_\infty \rightarrow \varepsilon_\infty^{\text{Au}}(\varepsilon_{\text{Si}})$.

Finally, we can also proceed in a similar way by analyzing the integrand for the case of ΔF_0 to prove that:

$$F_0^{(\text{FM})}(z) \approx \left(\frac{5}{3} - \frac{\pi}{4} \right) F_0^{(\text{PMC})}(z), \quad (\text{S.59})$$

corresponding to the result shown in Eq.(14) of the manuscript.

IV. FEATURES OF THE CASIMIR-POLDER FORCE FOR PMC SURFACE

A. The non-equilibrium Casimir-Polder force and the short-distance regime

In general scenarios for a nanoparticle in front of a plane surface, the non-equilibrium Casimir-Polder force is given by Eqs.(S.39)-(S.42). The expressions for the force can be re-cast in simple terms of Matsubara frequencies $\omega_n = 2\pi n k_B T/\hbar$. For the thermal factors, the hyperbolic cotangent in terms of its poles located at ω_n :

$$\coth\left(\frac{\hbar\omega}{2k_B T}\right) = \frac{2k_B T}{\hbar} \left[\frac{1}{\omega} + \sum_{n=1}^{+\infty} \left(\frac{1}{\omega + i\omega_n} + \frac{1}{\omega - i\omega_n} \right) \right]. \quad (\text{S.60})$$

In addition, we restrict to the case of full-bandwidth perfect conductors for simplicity, so $F_T \rightarrow 0$. We notice that \mathcal{R}_{PC} does not present poles in ω . By employing a contour enclosing the first quadrant of the complex plane, we have for the integrals of interest:

$$\begin{aligned} & \int_0^{+\infty} \frac{d\omega}{2\pi} \coth\left(\frac{\hbar\omega}{2k_B T}\right) \text{Re}[\alpha(\omega)] \mathcal{R}_{\text{PC}}(\omega, z) = \int_0^{+\infty} \frac{d\omega}{2\pi} \cot\left(\frac{\hbar\omega}{2k_B T}\right) \frac{[\alpha(i\omega) + \alpha^*(i\omega)]}{2} \mathcal{R}_{\text{PC}}(i\omega, z) \\ & + i \frac{k_B T}{2\hbar} \sum_{n=0}^{+\infty} (2 - \delta_{n,0}) \frac{[\alpha(i\omega_n) + \alpha^*(i\omega_n)]}{2} \mathcal{R}_{\text{PC}}(i\omega_n, z) + \frac{i}{2} \sum_{\nu_m^*} R_m[\alpha^*] \coth\left(\frac{\hbar\nu_m^*}{2k_B T}\right) \mathcal{R}_{\text{PC}}(\nu_m^*, z), \end{aligned} \quad (\text{S.61})$$

$$\begin{aligned} & \int_0^{+\infty} \frac{d\omega}{2\pi} \coth\left(\frac{\hbar\omega}{2k_B T}\right) \text{Im}[\alpha(\omega)] \mathcal{R}_{\text{PC}}(\omega, z) = \int_0^{+\infty} \frac{d\omega}{2\pi} \cot\left(\frac{\hbar\omega}{2k_B T}\right) \frac{[\alpha(i\omega) - \alpha^*(i\omega)]}{2i} \mathcal{R}_{\text{PC}}(i\omega, z) \\ & + \frac{k_B T}{2\hbar} \sum_{n=0}^{+\infty} (2 - \delta_{n,0}) \frac{[\alpha(i\omega_n) - \alpha^*(i\omega_n)]}{2} \mathcal{R}_{\text{PC}}(i\omega_n, z) - \frac{1}{2} \sum_{\nu_m^*} R_m[\alpha^*] \coth\left(\frac{\hbar\nu_m^*}{2k_B T}\right) \mathcal{R}_{\text{PC}}(\nu_m^*, z), \end{aligned} \quad (\text{S.62})$$

with $R_m[\alpha^*] = \text{Res}[\alpha^*(\omega), \nu_m^*]$, with ν_m the poles of the polarizability $\alpha(\omega)$ as mentioned in the previous section. Notice that this calculations are valid for arbitrary scenarios (different temperatures). Employing the last expressions, we can write the Casimir-Polder force as for a PEC (PMC) surface:

$$F_z(z) = \pm [F_{\text{St}}(z, T_{\text{EM}}) + F_{\text{Env}}(z, T_{\text{EM}}) + F_{\text{Mat}}(z, T_{\text{EM}}, T_{\text{NP}}) + F_{\text{Rad}}(z, T_{\text{NP}})], \quad (\text{S.63})$$

with the different contributions given by:

$$F_{\text{St}}(z, T_{\text{EM}}) = -\frac{3k_B T_{\text{EM}}}{16\pi z^4} \alpha_0, \quad (\text{S.64})$$

$$F_{\text{Env}}(z, T_{\text{EM}}) = \frac{k_B T_{\text{EM}}}{\hbar} \sum_{n=1}^{+\infty} \frac{[\alpha(i\omega_n) + \alpha^*(i\omega_n)]}{2} \mathcal{R}(i\omega_n, z), \quad (\text{S.65})$$

$$F_{\text{Mat}}(z, T_{\text{EM}}, T_{\text{NP}}) = \sum_{\nu_m^*} \text{Re} \left[R_m[\alpha^*] \left(\mathcal{N} \left[\frac{\hbar \nu_m^*}{k_B T_{\text{EM}}} \right] - \mathcal{N} \left[\frac{\hbar \nu_m^*}{k_B T_{\text{NP}}} \right] \right) \mathcal{R}(\nu_m^*, z) \right], \quad (\text{S.66})$$

$$F_{\text{Rad}}(z, T_{\text{NP}}) = \frac{k_B T_{\text{NP}}}{\hbar} \sum_{l=1}^{+\infty} \frac{[\alpha(i\omega_l) - \alpha^*(i\omega_l)]}{2} \mathcal{R}(i\omega_l, z), \quad (\text{S.67})$$

where $\alpha_0 \equiv \alpha(0)$ stands for the static polarizability, the Matsubara $\omega_n = 2\pi n k_B T_{\text{EM}}/\hbar$ while $\omega_l = 2\pi l k_B T_{\text{NP}}/\hbar$, and with $\mathcal{N}(x) = 1/(\text{Exp}[x] - 1)$.

First, the contribution corresponding to F_{St} stands for the thermal Casimir-Polder force between the surface and the nanoparticle. This contribution is independent of the material of the plate and depends only on the static value of the polarizability (α_0), while it depends on the temperature of the environmental EM field T_{EM} . Secondly, F_{Env} corresponds to the contribution of the environmental EM field including the dynamical properties of the nanoparticle and also the characteristics of the plate. This contribution is responsible of the Casimir-Polder force at thermal equilibrium at zero temperature and the fact that depends on the combination $\alpha + \alpha^*$ resembles the fact that depends on the real part of the polarizability which is associated to the dispersive properties of the nanoparticle. This is consistent with the fact that this contribution depends on the temperature of the environmental EM field, which is dispersed by the nanoparticle. The contribution F_{Mat} stands for a purely non-equilibrium contribution since at equilibrium $F_{\text{Mat}}(z, T, T) = 0$ for arbitrary T . Including the information of the poles of the polarizability, this contribution is characterized by the plasmonic frequencies $\text{Re}(\nu_m)$ of the material nanoparticle. Lastly, the contribution in F_{Rad} stands for a force associated to the radiation of the nanoparticle. The fact that depends on the combination $\alpha - \alpha^*$ resembles the fact that depends on the imaginary part of the polarizability which is associated to the dissipative (absorption and emission) properties of the nanoparticle. This is consistent with the fact that this contribution depends on the temperature of the nanoparticle.

Finally, notice that in thermal equilibrium ($T_{\text{EM}} = T_{\text{NP}} \equiv T$), the expression simplifies to:

$$\begin{aligned} F_z^{\text{Eq}}(z) &= \pm [F_{\text{St}}(z, T) + F_{\text{Env}}(z, T) + F_{\text{Rad}}(z, T)] \\ &= \pm \left[-\frac{3k_B T_{\text{EM}}}{16\pi z^4} \alpha_0 + \frac{k_B T_{\text{EM}}}{\hbar} \sum_{n=1}^{+\infty} \alpha(i\omega_n) \mathcal{R}_{\text{PC}}(i\omega_n, z) \right], \end{aligned} \quad (\text{S.68})$$

which for the PEC case stands for the typical Casimir-Polder force at thermal equilibrium.

For a SiC nanoparticle of radius $R = 50\text{nm}$ in front of a PMC surface, we show in Fig.2 the equilibrium Casimir-Polder force for different temperatures. We can clearly observe that for $z < 1\mu\text{m}$ (or in the short-distance regime defined by $k_B T z / [\hbar c] \ll 1$) all the curves are almost the same for a broad range of temperature values. In this sense, it is verified that in the short-distance regime we have $F_z(z) \approx F_0(z)$ as mentioned in the manuscript.

B. Force on SiC, Au and Si nanoparticles

The Casimir-Polder force for the PMC plane depends on the nanoparticle's polarizability according to Eq.(S.68). We consider the levitation of SiC, Au and Si nanoparticles. For SiC we employed a permittivity model $\varepsilon_{\text{SiC}}(\omega) = \varepsilon_\infty(\omega_L^2 - \omega^2 - i\gamma\omega)/(\omega_T^2 - \omega^2 - i\gamma\omega)$, where $\omega_L = 18.253 \times 10^{13}\text{s}^{-1}$, $\omega_T = 14.937 \times 10^{13}\text{s}^{-1}$, $\gamma = 8.966 \times 10^{11}\text{s}^{-1}$ and

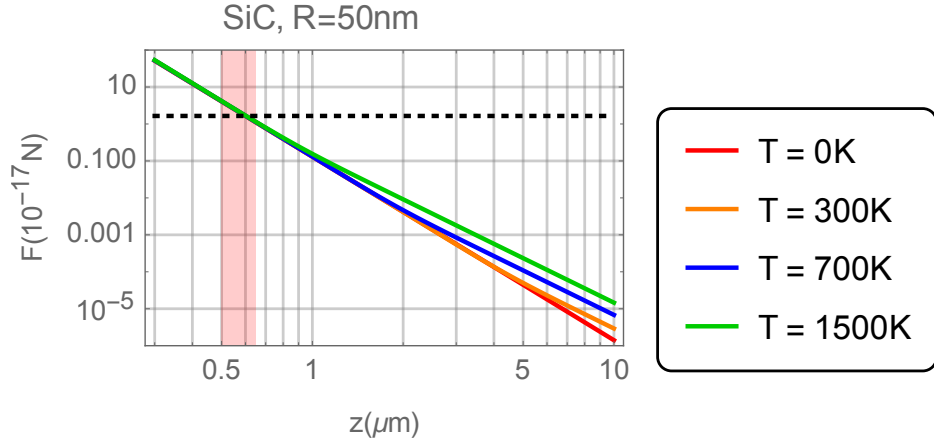


FIG. 2: Casimir-Polder for acting on a SiC nanoparticle with $R = 50\text{nm}$ radius in front of a PMC plane surface and held at equilibrium for temperature values $T = 0\text{K}, 300\text{K}, 700\text{K}, 1500\text{K}$, according to Eq.(S.53) (with $b = 0$ and no cutoffs) and Eq.(S.68). The black dotted horizontal line corresponds to the modulus of the nanoparticle's weight force mg . The intersections between the weight and the different curves give the levitation position for each case. The red shaded region corresponds to an approximate region $0.5\text{-}0.65\mu\text{m}$ corresponding to the levitation of SiC nanoparticles in front of broadband PMCs.

$\epsilon_\infty = 6.7$. For Au we take $\epsilon_{\text{Au}}(\omega) = \epsilon_\infty^{\text{Au}} - \omega_{\text{Pl}}^2/(\omega^2 + i\gamma_{\text{Au}}\omega)$, with $\omega_{\text{Pl}} = 2.15 \times 10^{15}\text{s}^{-1}$, $\gamma_{\text{Au}} = 5.88 \times 10^{13}\text{s}^{-1}$ and $\epsilon_\infty^{\text{Au}} = 5$. For Si we used a constant permittivity $\epsilon_{\text{Si}} = 12.25$ (corresponding to a refraction index of 3.5). The mass densities for each material are $\rho_{\text{SiC}} = 3210\text{Kg/m}^3$, $\rho_{\text{Au}} = 19300\text{Kg/m}^3$, $\rho_{\text{Si}} = 2330\text{Kg/m}^3$. In Fig.3 we show the comparison between the Casimir-Polder forces and the weights corresponding to these types of material nanoparticles. The intersections of a colored curve with the respective dotted horizontal lines corresponds to the equilibrium points.

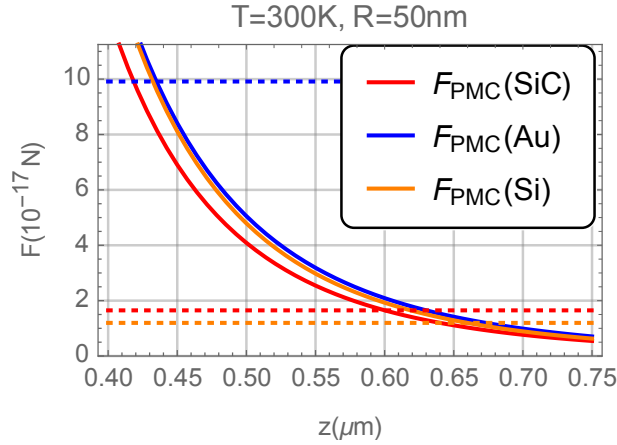


FIG. 3: Equilibrium Casimir-Polder forces at $T = 300\text{K}$ for SiC (red lines), Au (blue lines) and Si (orange lines) nanoparticles in front of PEC and PMC surfaces. The curves correspond to Eq.(S.68), which at the short-distances regime also corresponds to Eq.(S.53) with $b = 0$. Solid curves correspond to the interaction with PMC surfaces, while dashed curves correspond to PEC surfaces. Dotted horizontal lines corresponds to the weights of each nanoparticle.

For SiC the equilibrium occurs at $z_{\text{SiC}} = 600\text{nm}$, for Au we have $z_{\text{Au}} = 440\text{nm}$ and for Si $z_{\text{Si}} = 660\text{nm}$.

* Electronic address: adrianrubioloquez0102@gmail.com

† URL: <http://www.GianniniLab.com>

¹ C. Henkel, K. Joulain, J.-P. Mulet and J.-J. Greffet, *J. Opt. A: Pure Appl. Opt.* **4** (2002) S109-S114.

² S. Buhmann, *Dispersion Forces I: Macroscopic Quantum Electrodynamics and Ground-State Casimir, Casimir-Polder and van der Waals Forces* (Springer-Verlag, Berlin, Germany, 2012).